Fluorescence Energy Transfer to Dye-Labeled DNA from a Conjugated Polyelectrolyte Prequenched with a Water-Soluble C_{60} Derivative

Huaping Li, Renqiang Yang, and Guillermo C. Bazan*

Department of Materials and Chemistry & Biochemistry, Institute for Polymers and Organic Solids, University of California, Santa Barbara, California 93106

Received September 18, 2007; Revised Manuscript Received December 7, 2007

ABSTRACT: The emission of the cationic polyelectrolyte poly[9,9′-bis(6″-*N*,*N*,*N*-trimethylammonium)hexyl)-fluorene-*alt*-4,7-(2,1,3-benzothiadiazole) dibromide] (PFBT) is effectively quenched via photoinduced electron transfer by the negatively charged C_{60} derivative sodium diphosphorate methano[60]fullerene (SDPMF). Stern−Volmer analysis shows the quenching constant as high as 2.8×10^{12} M^{-1}, consistent with the formation of ground state complexes. Addition of Cy5-labeled ssDNA to PFBT leads to concurrent FRET to Cy5 and a quenching of PFBT emission that is intrinsic to the addition of ssDNA. Similar experiments carried out with a solution of PFBT that was prequenched with SDPMF result in a stable PFBT background emission and a clearly observed Cy5 emission rise. These observations were applied to ssDNA assays that take advantage of Cy5-labeled PNA. The result is a FRET-based detection method with more stable and readily quantifiable optical signals.

Introduction

Conjugated polyelectrolytes (CPEs)[1] constitute a class of materials that combine the optical and semiconducting properties[2] of polymers containing a delocalized electronic structure with the ability of polyelectrolytes[3] to form complexes,[4] change coil conformation,[5] and adsorb to surfaces[6] via electrostatic interactions. Their structures allow incorporation into optoelectronic devices where oxidation (hole injection) and reduction (electron injection) of their backbones can be compensated by the associated ions.[7] Their solubility in polar solvents allows fabrication of multilayer polymer-based devices[8] in which the barriers of charge injection are lowered, relative to neutral conjugated polymers, presumably via a mechanism that involves modification of the effective work function of the metal because of the presence of dipoles.[9,10]

CPEs can also be water-soluble, and this property allows their use in biological assays where optical amplification of fluorescent signals can be achieved by virtue of their light-harvesting capabilities.[11] In one particular strategy, selectivity is achieved by orchestrating electrostatic interactions so that close proximity between the CPEs and a probe with a signaling dye occurs only after a specific molecular recognition event.[12] This general approach has been used to detect a variety of targets, including DNA,[13] RNA,[14,15] and proteins.[16] Other detection methods involve the electrostatic binding of CPEs to a surface when a specific recognition event changes the surface charge,[17] the recovery of quenched emission via a specific recognition process,[18] and changes in chain conformation induced by complex formation.[19] Nonspecific contacts between nontarget species and the hydrophobic CP backbone are complex and need special attention for attaining selectivity, as these interactions can easily lead to misinterpretation of results.[20]

Optical studies of CPEs as a function of different environments yield insight into self-assembly processes important for biological assays and, more generally, for understanding the forces that coordinate the organization of π-conjugated molecules and materials.[21,22] There are substantial gaps in our knowledge, for example, on the structure and internal organization of aggregates containing CPEs and oppositely charged biological molecules.[23] The distance and orientation of the optical components in these aggregates bear an influence on processes such as fluorescence resonance energy transfer (FRET), photoinduced charge transfer, and the self-quenching of the CPEs and optical reporters.[24,25] Even with well-defined charged oligomers, one finds large differences in optical performance as a function of small perturbations such as the presence of small quantities of surfactants.[26] Despite these complexities, there continues to be substantial progress in the development of CPE-based biosensors.[11,27]

In this contribution, we report on the efficient fluorescence quenching of the cationic polymer poly[9,9′-bis(6″-*N*,*N*,*N*-trimethylammonium)hexyl)fluorene-*alt*-4,7-(2,1,3-benzothiadiazole) dibromide] (PFBT, see Scheme 1) with the negatively charged C_{60} derivative, sodium diphosphorate methano[60]-fullerene (SDPMF). Such quenching was anticipated on the basis of extensive prior work on neutral conjugated polymers that demonstrated photoinduced electron transfer to the electron deficient C_{60} framework.[28] Starting with the nonemissive PFBT/SDPMF complexes, it is possible to sensitize the emission of dye-labeled single-stranded DNA (ssDNA) or duplexes containing ssDNA/labeled PNA (PNA = peptide nucleic acid)[29] upon excitation of PFBT, presumably via a process that involves displacement of SDPMF from the proximity of the polymer backbone. The overall process reduces residual background signal from the sensitizing polymer, thereby providing an opportunity to simplify signal processing in functioning assays.

Results and Discussion

UV−Vis Absorption and Photoluminescence Spectroscopy. Figure 1 shows the normalized UV−vis absorption and photoluminescence (PL) spectra of SDPMF, PFBT, and a ssDNA strand modified with the Cy5 reporter dye ($ssDNA_1$-Cy5). The specific sequence of $ssDNA_1$-Cy5 is 5′-Cy5-ACT

* Corresponding author. E-mail: bazan@chem.ucsb.edu.

10.1021/ma702102v CCC: $40.75
Published on Web 01/24/2008

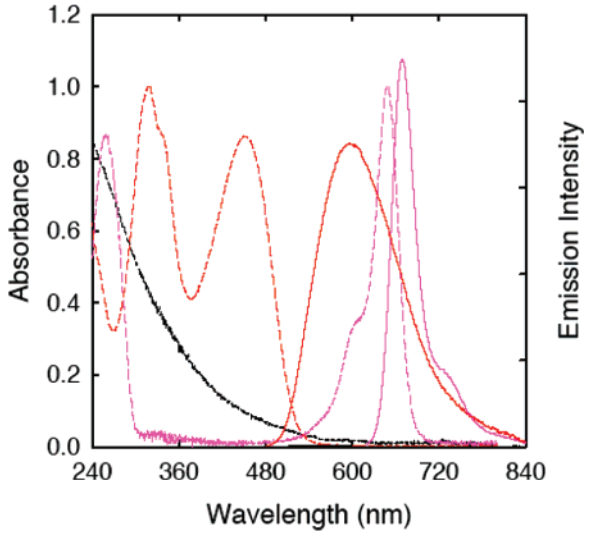

Figure 1. Spectroscopic properties. Normalized UV−vis absorption (dashed lines) and PL (solid lines) spectra of SDPMF (black, 6.2×10^{-5} M), PFBT (red, 6.1×10^{-5} M), and 5′-Cy5-ACT TTG ACT ATG TGG GTG CT-3′ (pink, 6.8×10^{-6} M, in terms of DNA repeat units, i.e., bases) in phosphate buffer (50 mM, pH 7.4).

Scheme 1. Molecular Structures of PFBT and SDPMF

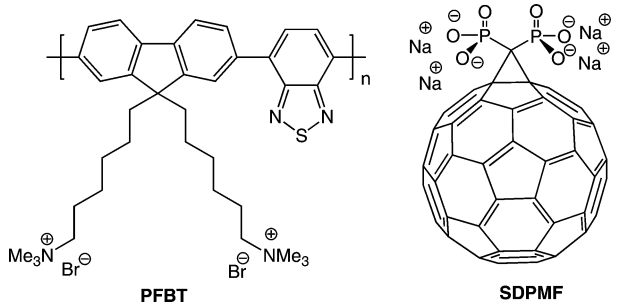

TTG ACT ATG TGG GTG CT-3′. All spectral measurements were done in a sodium phosphate buffer solution, unless otherwise indicated. SDPMF displays a featureless monotonic absorption curve and a very weak and broad PL spectrum in the 400−700 nm range, with a quantum yield of $\sim 10^{-4}$.[30]

Equation 1[31] describes how the FRET rate ($k_{t(r)}$) changes as a function of the donor−acceptor distance (r), the orientation factor (κ), and the overlap integral ($J(\lambda)$), which expresses the spectral overlap between the donor emission and the acceptor absorption.[32]

$$k_{t(r)} \propto \frac{1}{r^6} \kappa^2 J(\lambda) \qquad (1)$$

As shown in Figure 1, the overlap between the emission of PFBT and the absorbance of Cy5 in the 480−720 nm range satisfies the $J(\lambda)$ requirement in eq 1. However, the emission band of PFBT is much broader than that of Cy5, resulting in overlap in the range of 620−840 nm. From these considerations we anticipated an allowed FRET process that would lead to difficulties in the deconvolution of signals from the donor and acceptor components.

Before examining in detail the FRET characteristics of the PFBT/Cy5 system, we probed the fluorescence quenching abilities of SDPMF. As shown in Figure 2a, the addition of SDPMF to solutions of PFBT ([RU] = 3.2×10^{-6} M, where RU corresponds to the repeat unit of the polymer) results in a progressive decrease in the PL intensity. These PL spectra were measured after 5 min of mixing. There are no further changes in the spectral characteristics of the solution after this time, even after several hours of standing inside a cuvette. The volume of the SDPMF solution added to generate Figure 2a is sufficiently small that the change in [RU] throughout the quenching studies is less than 1%. Changes in PL intensities are therefore not due to a decrease of absorption. The PFBT emission is quenched by ~90% with [SDPMF] = 5.0×10^{-12} M and is almost absent when [SDPMF] = 2.5×10^{-11} M. Normalization of the PFBT spectra in the presence and absence of SDPMF reveals no changes in the shape of the emission band.

PL quenching efficiencies can be quantified by using Stern−Volmer analysis,[33] as shown by eq 2:

$$I_0/I = 1 + K_{SV}[Q] \qquad (2)$$

where I_0 and I are the fluorescence intensities in the absence and presence of quencher, respectively, and [Q] is the quencher concentration. The Stern−Volmer constant, K_{SV}, provides a direct measure of the quenching efficiency and is determined from the linear portion of a plot of I_0/I vs [Q]. Figure 2b shows the Stern−Volmer plot for PFBT using SDPMF as the quenching agent. From the slope of Figure 2b in the concentration of 0−2.5 pM and eq 2, one obtains $K_{SV} = 2.8 \times 10^{12}$ M^{-1}. From the emission lifetime (τ_0) of PFBT in the absence of SDPMF ($\tau_0 \sim 0.5$ ns) and using the relationship for K_{SV} in a dynamic process ($K_{SV} = k_q\tau_0$), one obtains an estimate for the bimolecular quenching constant (k_q) of $\sim 5 \times 10^{21}$ $(M\ s)^{-1}$, which is far too large for a collisional process. The K_{SV} for PFBT/SDPMF is 4 orders of magnitude larger than those observed when micromolar concentrations of cationic poly(*p*-phenylene) and poly(arylene ethynylene) polymers are quenched by anionic inorganic complexes [34,35] and anionic naphthalene diimides[36] and is even greater than the reported quenching of cationic poly(fluorene)s by gold nanoparticles.[37]

That the K_{SV} for the emission quenching of PFBT by SDPMF is too large for a collisional process allows us to infer the formation of ground state complexes. The magnitude of K_{SV} reflects a combination of effects: (a) a highly efficient photoinduced electron transfer from photoexcited PFBT (electron donor) to C_{60} (electron acceptor), (b) exciton migration among the PFBT optically active units, and (c) a large equilibrium constant favoring PFBT/SDPMF aggregation. The PFBT/SDPMF Stern−Volmer plots deviate downward from linearity when [SDPMF] > 2.5×10^{-12} M. Such behavior is in contrast to previously observed upward curvatures in other conjugated polyelectrolyte/quencher systems where a crossover from static quenching to sphere of action quenching mechanisms has been proposed.[38] The point of departure from linear behavior depends on experimental conditions and, most importantly, on the initial [PFBT]. The end result is that the K_{SV} values show substantial variations, as they are determined from a fairly narrow concentration range at the initial stages of quenching by SDPMF. Variations in quenching are also expected on the basis of the internal composition of ground state complexes containing conjugated polyelectrolytes.[39] However, when one looks at the magnitude of the calculated K_{SV} values, they unambiguously indicate very efficient quenching.

Debye−Hückel theory[40] predicts that the Debye screening length decreases at high ionic strengths so that complexation by electrostatic attraction is less favorable.[37,38] For the PFBT/SPDMF system, the association constant would decrease under circumstances where electrostatic attraction between the oppositely charged groups provides at least part of the aggregation driving force. To probe this issue, Stern−Volmer plots for the emission quenching of PFBT ([RU] = 3.2×10^{-6} M) with

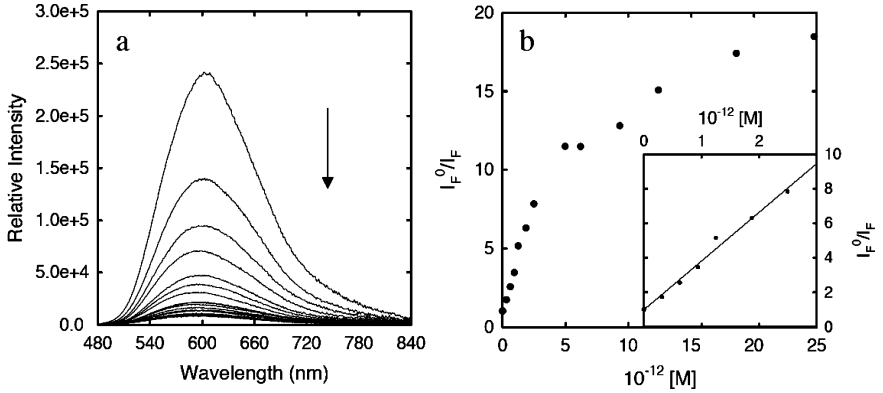

Figure 2. Addition of SDPMF results in effective quenching of the PFBT emission. (a) PL spectra of PFBT ([RU] = 3.2×10^{-6} M, λ_{exc} = 330 nm) as a function of [SDPMF]: 0, 3.1×10^{-13}, 6.2×10^{-13}, 9.4×10^{-13}, 1.2×10^{-12}, 1.9×10^{-12}, 2.5×10^{-12}, 5.0×10^{-12}, 6.2×10^{-12}, 9.3×10^{-12}, 1.2×10^{-11}, 1.9×10^{-11}, and 2.5×10^{-11} M. (b) Stern−Volmer plot for [SDPMF] = $0-2.5 \times 10^{-12}$ M; inset shows the linear regime from which K_{SV} is calculated.

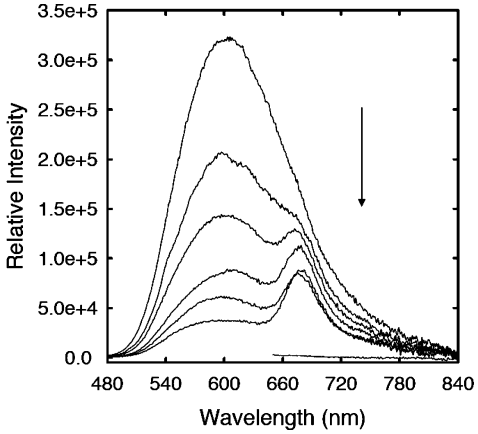

Figure 3. Addition of ssDNA$_1$-Cy5 results in the appearance of Cy5 emission at expense of the PFBT emission. PL spectra of PFBT ([RU] = 3.2×10^{-6} M, λ_{exc} = 330 nm) after addition of ssDNA-Cy5 in the concentrations of 0, 1.7×10^{-10}, 3.4×10^{-10}, 5.1×10^{-10}, 6.9×10^{-10}, and 8.6×10^{-10} M. The PL spectrum of the final solution upon direct Cy5 excitation at 640 nm is shown as the lowest intensity spectrum from ~655 to 840 nm.

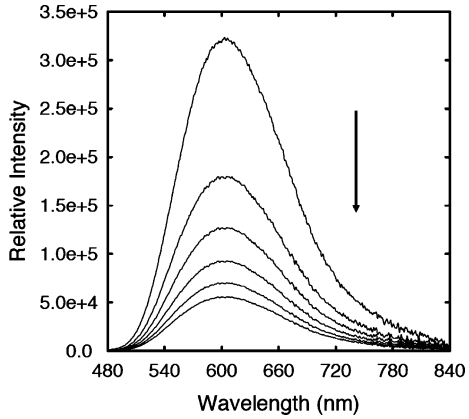

Figure 4. Decrease of the PFBT emission intensity ([RU] = 3.2×10^{-6} M, λ_{exc} = 330 nm) upon addition of ssDNA$_2$: 0, 1.7×10^{-10}, 3.4×10^{-10}, 5.1×10^{-10}, 6.9×10^{-10}, and 8.6×10^{-10} M.

SDPMF were carried out in sodium phosphate buffer, except that an additional 0.075 M of NaCl was added. These conditions led to a K_{SV} value of ~1.1×10^{10} M^{-1}, i.e., a reduction of ~2 orders of magnitude compared to that obtained under the conditions in Figure 2. The decrease in quenching efficiency by the presence of the additional NaCl indicates that the complexation between PFBT and SDPMF is mediated to a significant extent by electrostatic attraction between the two partners. Hydrophobic effects also are likely to contribute to the association constant, as shown for previous conjugated polyelectrolyte materials.[41]

FRET to ssDNA-Cy5 from PFBT Prequenched with SDPMF. A series of experiments were performed to study how SDPMF quenching influences the energy transfer efficiency from PFBT to ssDNA$_1$-Cy5. We first examined the changes in PL spectra of PFBT as a function of [ssDNA$_1$-Cy5] (in terms of bases), and the results are shown in Figure 3. The general mechanism involves electrostatic complexation between the oppositely charged polyelectrolytes, which brings together the optically active PFBT and Cy5 units into close proximity and satisfies the distance requirement for FRET in eq 1. While the association is similar to that between PFBT and SDPMF, the difference in orbital energy levels of the two acceptors leads to different events. For Cy5 one would anticipate FRET, whereas for the more electron-deficient SDPMF, photoinduced electron transfer is preferred.[42] Figure 3 shows a decrease of the PFBT emission as ssDNA$_1$-Cy5 is added. The rise of the Cy5 emission is also observed, initially as a shoulder on the stronger and broader PFBT band and then as a more clearly defined band at 672 nm. Once 8.6×10^{-10} M of ssDNA$_1$-Cy5 is added, further additions result in no additional increase. The drop in the residual PFBT emission at 672 nm thus compensates increases in Cy5 emission. Figure 3 also shows that the emission obtained from a solution of PFBT and ssDNA$_1$-Cy5 when [ssDNA$_1$-Cy5] = 8.6×10^{-10} M upon direct excitation of Cy5 at 640 nm is negligible. The strong Cy5 emission observed only when PFBT is excited is thus a direct consequence of excitation transfer via FRET and the larger optical density of PFBT.

When looking at Figure 3, one observes that the emission of Cy5 at the saturation point is considerably weaker than the initial PFBT emission. Since the fluorescence quantum efficiency of PFBT (7%) is much lower than that of Cy5 (21%), at least when one measures the performance of these chromophores prior to PFBT/ssDNA-Cy5 complexation, not all of the initial excitations on PFBT are transferred to Cy5 via FRET. Another process must therefore be present. To dissect the different optical processes involved in PFBT/ssDNA$_1$-Cy5 complexation, perturbations of PFBT emission by *unlabeled* ssDNA were examined by looking at the PL spectra upon addition of ssDNA$_2$ (5′-CAG CTT GAC T-3′). As shown in Figure 4, the PL of PFBT decreases upon the addition of ssDNA$_2$ from 0 to 8.6×10^{-10} M (in terms of bases). When 8.6×10^{-10} M of ssDNA$_2$ is added, one observes ~80% quenching of the original emission. Although the length of ssDNA$_2$ is shorter than that

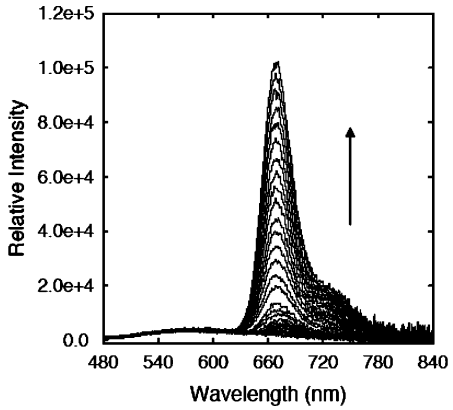

Figure 5. Emergence of the Cy5 emission is more clearly observed when the emission of PFBT is prequenched by SDPMF. PL spectra of PFBT ([RU] = 3.2×10^{-6} M, $\lambda_{exc} = 330$ nm) with 2.5×10^{-11} M of SDPMF after addition of ssDNA-Cy5 in the concentrations of 0, 1.7×10^{-10}, 3.4×10^{-10}, 6.9×10^{-10}, 1.0×10^{-9}, 1.7×10^{-9}, 2.3×10^{-9}, 5.8×10^{-9}, 9.0×10^{-9}, 1.3×10^{-8}, 1.9×10^{-8}, 2.6×10^{-8}, 3.6×10^{-8}, 5.3×10^{-8}, 7.0×10^{-8}, 8.7×10^{-8}, 1.0×10^{-7}, 1.2×10^{-7}, 1.4×10^{-7}, 1.5×10^{-7}, 1.7×10^{-7}, 1.9×10^{-7}, and 2.1×10^{-7} M.

of $ssDNA_1$, it is unambiguous that complexation with PFBT leads to a reduction of emission efficiency. Thus, the decrease of PFBT emission in Figure 3 is a combination of FRET to Cy5 and a quenching process that is intrinsic to its complexation with ssDNA. The mechanism of the latter is likely due to self-quenching upon close association of polymer chains in the PFBT/ssDNA aggregate and possibly photoinduced electron transfer to the guanine bases.[43−45]

Figure 5 shows the changes in the PL spectra obtained when $ssDNA_1$-Cy5 is added to a solution of PFBT previously treated with SDPMF. The initial conditions were chosen so that the PFBT emission is essentially quenched. There is a clear emergence of Cy5 emission as $ssDNA_1$-Cy5 is added. In contrast to Figure 3, there are no variations in the intensity from the residual PFBT band. Moreover, the concentration range (1.7×10^{-10}−2.1×10^{-7} M) of added $ssDNA_1$-Cy5 responsive to sensitization via FRET with the prequenched PFBT solution extends beyond that which can be probed with a pristine PFBT solution (1.7×10^{-10}−8.6×10^{-10} M). However, the net Cy5 emission intensities in the presence of SDPMF at similar ssDNA-Cy5 concentrations are lower. For example, the Cy5 emission intensity with [$ssDNA_1$-Cy5] = 6.9×10^{-10} M is ∼5 times weaker than that obtained with a pristine PFBT solution. This decrease in intensity is likely a combination of quenching of PFBT by SDPMF prior to FRET and possible direct quenching of Cy5 by SDPMF.

Applications of SDPMF Quenched PFBT in ssDNA Detection Protocols. In previous work,[12] a ssDNA sensory process was developed that comprises two components: (a) a light-harvesting cationic conjugated polyelectrolyte and (b) a probe oligonucleotide consisting of a PNA labeled with a reporter fluorophore. Addition to the solution of ssDNA of a sequence complementary to the PNA strand yields the duplex structure. Electrostatic interactions bring the conjugated polyelectrolyte into close proximity to the negatively charged PNA/ssDNA duplex, resulting in FRET from the polymer to the signaling chromophore. When a nontarget polynucleotide is added, complexation between the cationic polymer and the probe PNA does not occur. Under these circumstances the signaling dye remains bound to a neutral macromolecule; there is no electrostatic binding of the fluorophore-tagged PNA to the conjugated polyelectrolyte, and the average distance between the optical partners is too large for effective FRET. It is possible to differentiate complementary and noncomplentary ssDNA by exciting the polymer and measuring the reporter fluorophore emission.

The general procedure described above was implemented using a Cy5-labeled PNA probe (PNA-Cy5, Cy5-NH_2-OO-CCG TGC CCA GTG AG, where "OO" refers to an 8-amino-3,6-dioxooctanoic acid linker) and PFBT with and without SDMF. Conditions included the use of 5% 1-methylpyrrolidinone in phosphate buffer to reduce nonspecific hydrophobic interactions.[12] Complementary ($ssDNA_C$, 5′-TAC GCT GCA GTC CTC GCT CAC TGG GCA CGG-3) and noncomplementary ($ssDNA_{NC}$, 5′-CAG CTT GAC TCA GCT TGA CTC AGC TTG ACT-3′) ssDNAs (5.0×10^{-8} M) were mixed with PNA-Cy5 (7.1×10^{-7} M) in phosphate buffer and shaken for 30 min at room temperature. The resulting solutions were subsequently added to a solution of PFBT or PFBT prequenched with SDPMF, and the PL spectra were measured.

Figure 6a shows the PL spectra obtained from a PFBT solution upon addition of PNA-Cy5 + $ssDNA_{NC}$. That no Cy5 emission is observed indicates the absence of FRET, consistent with the proposed mechanism of the assay and provides a good control experiment for testing complementary $ssDNA_C$. The decrease of PFBT emission in Figure 6a is similar to that shown in Figure 4 and is attributed to the quenching by $ssDNA_{NC}$. Emission from Cy5 upon excitation of PFBT is observed when hybridized PNA-Cy5/$ssDNA_C$ is added, as shown in Figure 6b. However, the main perturbation is the drastic decrease in PFBT emission.

Figure 6c shows that there are no significant changes in the PL spectra when a solution of PNA-Cy5 + $ssDNA_{NC}$ is added to PFBT pretreated with SDPMF. The PFBT:SPDMF stoichiometry of the starting solution was chosen to yield a decrease of PFBT emission by a factor of ∼300. Addition of $ssDNA_{NC}$ cannot further decrease the residual emission. It appears that any displacement of SDPMF by $ssDNA_{NC}$ exchanges quenching agents, resulting in no noticeable perturbations in the PL spectra, although the exact details are not fully understood at this stage. When a solution containing hybridized PNA-Cy5/$ssDNA_C$ is added (Figure 6d), the spectral response behaves as in Figure 5, where Cy5 emission emerges from the PFBT background. It is likely that this emission is a result of SDPMF displacement from the vicinity of PFBT by the negatively charged PNA-Cy5/ssDNA duplex. Comparison of parts b and d of Figure 6 highlights the advantage of pretreating the solution with SDPMF: one observes no variations in the background PFBT emission and a better defined emergence of the reporter dye. From a practical perspective, the signal at 672 nm *increases* when the target strand is present, a considerable advantage when compared to situations where the signal fluctuates considerably.

Conclusions

Highly effective quenching of PFBT emission can be achieved by addition of the anionic fullerene derivative SDPMF. Indeed, Stern−Volmer analysis indicates that the quenching efficiency is among the highest observed with conjugated polyelectrolytes. The mechanism of quenching is likely via a photoinduced electron transfer in ground state complexes in which electrostatic interactions play an important role in determining the association constant. Addition of unlabeled ssDNA causes a significant quenching of PFBT emission, probably as a result of self-quenching and charge transfer to the guanines bases. When ssDNA-Cy5 is added to PFBT, one observes a combination of effects: quenching of PFBT and FRET to Cy5. The end result is as in Figure 3, where large fluctuations in spectral response

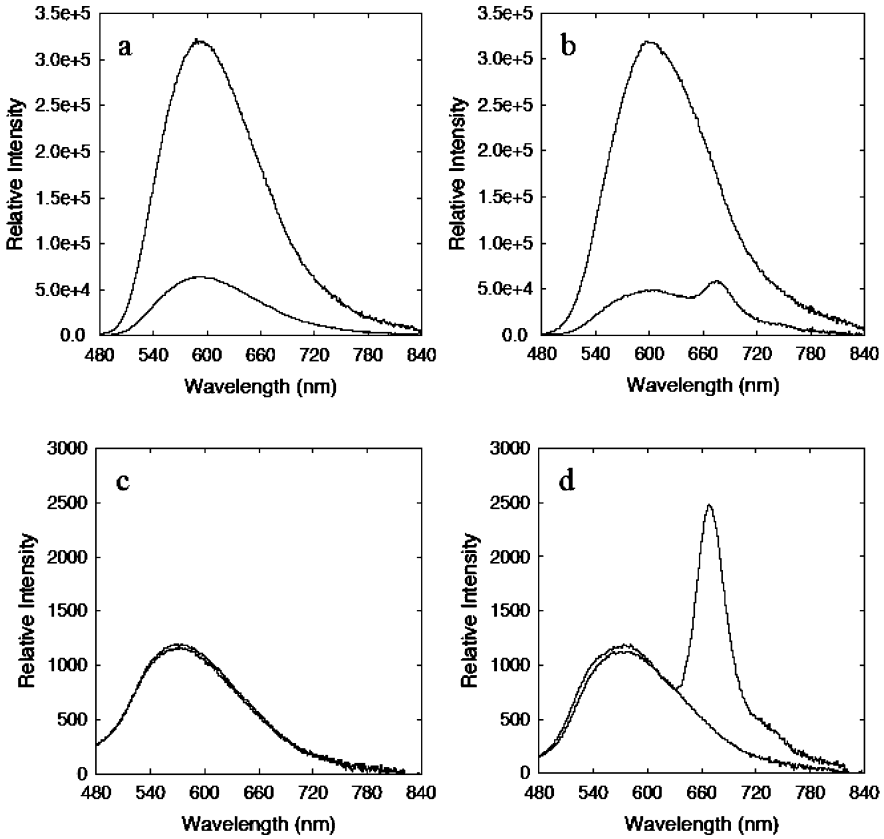

Figure 6. Prequenching with SDPMF results no variation of the donor emission and a better defined emergence of the acceptor Cy5 emission. PL spectra ($\lambda_{exc} = 330$ nm) of PFBT solutions (3.2×10^{-6} M) (a and b) and PFBT solutions prequenched by 2.5×10^{-11} M of SDPMF (c and d) upon addition of PNA-Cy5/ssDNA$_C$ (3.5×10^{-9} M/2.5×10^{-10} M in term of bases) (b and d) and PNA-Cy5 + ssDNA$_{NC}$ (3.5×10^{-9} M/2.5×10^{-10} M in term of bases) (a and c).

are observed. A significant simplification of the spectral response occurs when ssDNA-Cy5 is added to PFBT prequenched with SDPMF, as shown in Figure 5. There is a more clear observation of Cy5 emission under these conditions, and the spectra are responsive to a larger ssDNA-Cy5 concentration range. A disadvantage is the loss in net PL intensity.

The observations described above open the opportunity for controlling complexation events by electrostatic interactions to simplify the optical output in ssDNA-specific assays based on conjugated polyelectrolytes. Treating PFBT/SDPMF solutions with PNA-Cy5/ssDNA$_{NC}$ leads to no perturbations in the PL response, in contrast to the situation where only PFBT is used. Comparison of the results upon addition of PNA-Cy5/ssDNA$_C$ duplex shows that the signals of the assay are more easily interpreted with SDPMF-quenched PFBT. Thus, the control of optical properties in self-assembling systems via manipulation of electrostatic interactions provides a versatile tool for tailoring the response from biosensors based on conjugated polyelectrolytes.

Experimental Section

Materials. The synthesis, characterization, and photophysical properties of PFBT were previously reported.[17] SDPMF was synthesized and characterized following literature procedures.[46] 5′-Cy5-ACT TTG ACT ATG TGG GTG CT-3′ (ssDNA$_1$) and 5′-CAG CTT GAC T-3′ (ssDNA$_2$) were purchased from Integrated DNA Technologies, Inc. PNA-Cy5 (Cy5-NH$_2$-OO-CCG TGC CCA GTG AG) was purchased from Panagen; its complementary DNA (5′-TAC GCT GCA GTC CTC GCT CAC TGG GCA CGG-3′) and noncomplementary DNA (5′-CAG CTT GAC TCA GCT TGA CTC AGC TTG ACT-3′) ssDNAs were obtained from Integrated DNA Technologies, Inc. These materials were dissolved in potassium phosphate/sodium hydroxide buffer solution (50 mM, pH 7.4) purchased from Fisher Scientific Co., unless otherwise described.

Measurements. Fluorescence spectra were recorded on PTI (South Brunswick, NJ) Quantum Master fluorometer equipped with a xenon lamp light sources and a Hamamatsu (Middlesex, NJ) photomultiplier tube. The PL spectra of PFBT were measured from 480 to 840 nm with the excitation of 330 nm, employing a 385 nm cutoff filter to filter out the overtone of excitation light. The UV−vis absorption spectra were performed on a Shimadzu UV-2401 UV−vis spectrometer to calibrate the concentrations of ssDNA and PFBT.

Acknowledgment. We thank Dr. J. W. Hong for experimental assistance. Financial support from the Institute for Collaborative Biotechnologies and the NSF (DMR 0606414) is greatly appreciated.

References and Notes

(1) Pinto, M. R.; Schanze, K. S. *Synthesis* **2002**, *9*, 1293−1309.
(2) Hadziioannou, G.; van Hutten, P. F. *Semiconducting Polymers*; Wiley-VCH: Weinheim, 2000.
(3) Hara, M. *Polyelectrolytes: Science and Technology*; Marcel Dekker: New York, 1993.
(4) Liu, B.; Bazan, G. C. *Chem. Mater.* **2004**, *16*, 4467−4476.
(5) (a) Nilsson, K. P. R.; Rydberg, J.; Baltzer, L.; Inganas, O. *Proc. Natl. Acad. Sci. U.S.A.* **2003**, *100*, 10170−10174. (b) Ho, H. A.; Boissinot, M.; Bergeron, M. G.; Corbeil, G.; Dore, K.; Boudreau, D.; Leclerc, M. *Angew. Chem., Int. Ed.* **2002**, *41*, 1548−1551.
(6) Cutler, C. A.; Bouguettaya, M.; Reynolds, J. R. *Adv. Mater.* **2002**, *14*, 684−688.
(7) Edman, L.; Liu, B.; Vehse, M.; Swensen, J.; Bazan, G. C.; Heeger, A. J. *J. Appl. Phys.* **2005**, *98*, 044502.
(8) (a) Ma, W. L.; Iyer, P. K.; Gong, X.; Liu, B.; Moses, D.; Bazan, G. C.; Heeger, A. J. *Adv. Mater.* **2005**, *17*, 274−277. (b) Piok, T.; Plank, H.; Mauthner, G.; Gamerith, S.; Gadermaier, C.; Wenzl, F. P.; Patil, S.; Montenegro, R.; Bouguettaya, M.; Reynolds, J. R.; Scherf, U.;

Landfester, K.; List, E. J. W. *Jpn. J. Appl. Phys., Part 1* **2005**, *44*, 479−484. (c) Choi, K.; Zentel, R. *Macromol. Chem. Phys.* **2006**, *207*, 1870−1879. (d) Tseng, S. R.; Li, S. Y.; Meng, H. F.; Yu, Y. H.; Yang, C. M.; Liao, H. H.; Horng, S. F.; Hsu, C. S. *J. Appl. Phys.* **2007**, *101*, 084510.

(9) (a) Huang, F.; Hou, L. T.; Wu, H. B.; Wang, X. H.; Shen, H. L.; Cao, W.; Yang, W.; Cao, Y. *J. Am. Chem. Soc.* **2004**, *126*, 9845−9853. (b) Wu, H. B.; Huang, F.; Mo, Y. Q.; Yang, W.; Wang, D. L.; Peng, J. B.; Cao, Y. *Adv. Mater.* **2004**, *16*, 1826−1830.

(10) Yang, R. Q.; Wu, H. B.; Cao, Y.; Bazan, G. C. *J. Am. Chem. Soc.* **2006**, *128*, 14422−14423.

(11) Thomas, S. W.; Joly, G. D.; Swager, T. M. *Chem. Rev.* **2007**, *107*, 1339−1386.

(12) Gaylord, B. S.; Heeger, A. J.; Bazan, G. C. *Proc. Natl. Acad. Sci. U.S.A.* **2002**, *99*, 10954−10957.

(13) Gaylord, B. S.; Massie, M. R.; Feinstein, S. C.; Bazan, G. C. *Proc. Natl. Acad. Sci. U.S.A.* **2002**, *99*, 10954−10957.

(14) Liu, B.; Baudrey, S.; Jaeger, L.; Bazan, G. C. *J. Am. Chem. Soc.* **2004**, *126*, 4076−4077.

(15) Wang, S.; Bazan, G. C. *Adv. Mater.* **2002**, *14*, 1425−1428.

(16) (a) Pinto, M. R.; Schanze, K. S. *Proc. Natl. Acad. Sci. U.S.A.* **2004**, *101*, 7505−7510. (b) An, L. L.; Tang, Y. L.; Wang, S.; Li, Y. L.; Zhu, D. B. *Macromol. Rapid Commun.* **2006**, *27*, 993−997.

(17) (a) Liu, B.; Bazan, G. C. *Proc. Natl. Acad. Sci. U.S.A.* **2005**, *102*, 589−593. (b) Najari, A.; Ho, H. A.; Gravel, J. F.; Nobert, P.; Boudreau, D.; Leclerc, M. *Anal. Chem.* **2006**, *78*, 7896−7899. (c) Le, Floch, F.; Ho, H. A.; Harding-Lepage, P.; Bedard, M.; Neagu-Plesu, R.; Leclerc, M. *Adv. Mater.* **2005**, *17*, 1251−1254.

(18) Kumaraswamy, S.; Bergstedt, T.; Shi, X. B.; Rininsland, F.; Kushon, S.; Xia, W. S.; Ley, K.; Achyuthan, K.; McBranch, D.; Whitten, D. G. *Proc. Natl. Acad. Sci. U.S.A.* **2004**, *101*, 7511−7515.

(19) (a) Li, C.; Numata, M.; Takeuchi, M.; Shinkai, S. *Angew. Chem., Int. Ed.* **2005**, *44*, 6371−6374. (b) Le, Floch, F.; Ho, H. A.; Leclerc, M. *Anal. Chem.* **2006**, *78*, 4727−4731. (c) Aberem, M. B.; Najari, A.; Ho, H. A.; Gravel, J. F.; Nobert, P.; Boudreau, D.; Leclerc, M. *Adv. Mater.* **2006**, *18*, 2703−2707.

(20) Dwight, S. J.; Gaylord, B. S.; Hong, J. W.; Bazan, G. C. *J. Am. Chem. Soc.* **2004**, *126*, 16850−16859.

(21) Hoeben, F. J. M.; Jonkheijm, P.; Meijer, E. W.; Schenning, A. P. H. J. *Chem. Rev.* **2005**, *105*, 1491−1546.

(22) Wang, F. K.; Bazan, G. C. *J. Am. Chem. Soc.* **2006**, *126*, 15786−15792.

(23) Nilsson, K. P. R.; Inganäs, O. *Nat. Mater.* **2003**, *2*, 419−424.

(24) (a) Wang, S.; Gaylord, B. S.; Bazan, G. C. *J. Am. Chem. Soc.* **2004**, *126*, 5446−5451. (b) Xu, Q.-H.; Gaylord, B. S.; Wang, S.; Bazan, G. C.; Moses, D.; Heeger, A. J. *Proc. Natl. Acad. Sci. U.S.A.* **2004**, *101*, 11634−11639.

(25) Karlsson, K. F.; Åsberg, P.; Nilsson, K. P. R.; Inganäs, O. *Chem. Mater.* **2005**, *17*, 4204−4211.

(26) Gaylord, B. S.; Wang, S. J.; Heeger, A. J.; Bazan, G. C. *J. Am. Chem. Soc.* **2001**, *123*, 6417−6418.

(27) (a) Juan, Z.; Swager, T. M. *Adv. Polym. Sci.* **2005**, *177*, 151−179. (b) Pinto, M. R.; Tan, C.; Ramey, M. B.; Reynolds, J. R.; Bergstedt, T. S.; Whitten, D. G.; Schanze, K. S. *Res. Chem. Intermed.* **2007**, *33*, 79−90. (c) Vazquez, E.; Aguilar, A. E.; Moggio, I.; Arias, E.; Romero, J.; Barrientos, H.; Torres, J. R.; Vega, M. D. R. *Mater. Sci. Eng., C* **2007**, *27*, 787−793. (d) Shishkanova, T. V.; Volf, R.; Krondak, M.; Kral, V. *Biosens. Bioelctron.* **2007**, *22*, 2712−2717. (e) Garnier, F.; Bouabdallaoui, B.; Srivastava, P.; Mandrand, B.; Chaix, C. *Sens. Actuators, B* **2007**, *123*, 13−20. (f) Lopez-Cabarcos, E.; Retama, J. R.; Sholin, V.; Carter, S. A. *Polym. Int.* **2007**, *56*, 588−592. (g) Mikroyannidis, J. A.; Barberis, V. P. *J. Polym. Sci., Part A: Polym. Chem.* **2007**, *45*, 1481−1491. (h) Liu, B.; Bazan, G. C. *Chem. Asian J.* **2007**, *2*, 499−504. (i) Ambade, A. V.; Sandanaraj, B. S.; Klaikherd, A.; Thayumanavan, S. *Polym. Int.* **2007**, *56*, 474−481. (j) Gao, Z. Q.; Rafea, S.; Lim, L. H. *Adv. Mater.* **2007**, *19*, 602−606. (k) Lee, K.; Rouillard, J.-M.; Pham, T.; Gulari, E.; Kim, J. *Angew. Chem., Int. Ed.* **2007**, *46*, 4667−4670. (l) Liu, X. F.; Tang, Y. L.; Wang, L. H.; Zhang, J.; Song, S. P.; Fan, C.; Wang, S. *Adv. Mater.* **2007**, *19*, 1471−1474. (m) Duan, X. R.; Li, Z. P.; He, F.; Wang, S. *J. Am. Chem. Soc.* **2007**, *129*, 4154−4155.

(28) Sariciftci, N. S.; Smilowitz, L.; Heeger, A. J.; Wudl, F. *Science* **1992**, *258*, 1474−1476.

(29) (a) Nielsen, P. E., Egholm, M., Eds. *Peptide Nucleic Acids: Protocols and Applications*; Horizon Scientific Press: Portland, 1999. (b) Stender, H.; Fiandaca, M.; Hyldig-Nielsen, J. J.; Coull, J. *J. Microbiol. Methods* **2002**, *48*, 1−17.

(30) Kim, D.; Lee, M. *J. Am. Chem. Soc.* **1992**, *114*, 4429−4430.

(31) Förster, T. *Ann. Phys.* **1948**, *2*, 55−75.

(32) Lakowicz, J. R. *Principles of Fluorescence Spectroscopy*; Kluwer Academic/Plenum Publishers: New York, 1999.

(33) Stern, O.; Volmer, M. *Phys. Z.* **1919**, *20*, 183−188.

(34) Harrison, B. S.; Ramey, M. B.; Reynolds, J. R.; Schanze, K. S. *J. Am. Chem. Soc.* **2000**, *122*, 8561−8562.

(35) Huang, Y.-Q.; Fan, Q.-L.; Lu, X.-M.; Fang, C.; Liu, S.-J.; Yu-Wen, L.-H.; Wang, L.-H.; Huang, W. *J. Polym. Sci., Part A: Polym. Chem.* **2006**, *44*, 5788−5794.

(36) Zhao, X.; Pinto, M. R.; Hardison, L. M.; Mwaura, J.; Muller, J.; Jiang, H.; Witker, D.; Kleiman, V. D.; Reynolds, J. R.; Schanze, K. S *Macromolecules* **2006**, *39*, 6355−6366.

(37) Fan, C.; Wang, S.; Hong, J. W.; Bazan, G. C.; Plaxco, K. W.; Heeger, A. J. *Proc. Natl. Acad. Sci. U.S.A.* **2003**, *100*, 6297−6301.

(38) Wang, J.; Wang, D.; Miller, E. K.; Moses, D.; Bazan, G. C.; Heeger, A. J. *Macromolecules* **2000**, *33*, 5153−5158.

(39) Stork, M.; Gaylord, B. S.; Heeger, A. J.; Bazan, G. C. *Adv. Mater.* **2002**, *14*, 361−366.

(40) Israelachvili, J. *Intermolecular & Surface Forces*; Academic Press: London, 1992.

(41) Liu, B.; Gaylord, B. S.; Wang, S.; Bazan, G. C. *J. Am. Chem. Soc.* **2003**, *125*, 6705−6714.

(42) Cornil, J.; Lemaur, V.; Steel, M. C.; Dupin, H.; Burquel, A.; Beljonne, D.; Brédas, J. L. In *Organic Photovoltaics*; Sun, S. J., Sariciftci, N. S., Eds.; Taylor & Francis: Boca Raton, 2005.

(43) (a) Edman, L.; Mets, Ü.; Rigler, R. *Proc. Natl. Acad. Sci. U.S.A.* **1996**, *93*, 6710−6751. (b) Eggeling, C.; Fries, J. R.; Brand, L.; Gunther, R.; Seidel, C. A. M. *Proc. Natl. Acad. Sci. U.S.A.* **1998**, *95*, 1556−1561. (c) Lewis, F. D.; Wu, T.; Zhang, Y.; Letsinger, R. L.; Greenfield, S. R.; Wasielewski, M. R. *Science* **1997**, *277*, 673−676. (d) Lewis, F. D.; Letsinger, R. L.; Wasielewski, M. R. *Acc. Chem. Res.* **2001**, *34*, 159−170.

(44) Ho, P. K. H.; Kim, J. S.; Burroughes, J. H.; Becker, H.; Li, S. F. Y.; Brown, T. M.; Cacialli, F.; Friend, R. H. *Nature (London)* **2000**, *404*, 481−484.

(45) Seidel, C. A. M.; Schulz, A.; Sauer, M. H. M. *J. Phys. Chem.* **1996**, *100*, 5541−5553.

(46) Cheng, F.; Yang, X.; Fan, C.; Zhu, H. *Tetrahedron* **2001**, *57*, 7331−7335.

MA702102V